













# Predicting leaf traits across functional groups using reflectance spectroscopy

Shan Kothari<sup>1</sup> , Rosalie Beauchamp-Rioux<sup>1</sup> , Florence Blanchard<sup>1</sup>, Anna L. Crofts<sup>2</sup> , Alizée Girard<sup>1</sup>, Xavier Guilbeault-Mayers<sup>1</sup> , Paul W. Hacker<sup>3</sup> , Juliana Pardo<sup>1</sup> , Anna K. Schweiger<sup>1,4</sup> , Sabrina Demers-Thibeault<sup>1</sup>, Anne Bruneau<sup>1</sup> , Nicholas C. Coops<sup>3</sup> , Margaret Kalacska<sup>5</sup> , Mark Vellend<sup>2</sup>  and Etienne Laliberté<sup>1</sup> 

<sup>1</sup>Département de Sciences Biologiques, Institut de Recherche en Biologie Végétale, Université de Montréal, 4101 Sherbrooke Est, Montréal, QC H1X 2B2, Canada; <sup>2</sup>Département de Biologie, Université de Sherbrooke, Sherbrooke, QC J1K 2X9, Canada; <sup>3</sup>Department of Forest Resources Management, University of British Columbia, Vancouver, BC V6T 1Z4, Canada; <sup>4</sup>Department of Geography, University of Zurich, Zürich 8057, Switzerland; <sup>5</sup>Department of Geography, McGill University, Montréal, QC H3A 0B9, Canada

## Summary

Author for correspondence:

Shan Kothari

Email: [shan.kothari@umontreal.ca](mailto:shan.kothari@umontreal.ca)

Received: 6 July 2022

Accepted: 30 October 2022

New Phytologist (2023) 238: 549–566

doi: 10.1111/nph.18713

**Key words:** foliar chemistry, functional traits, leaf economics, partial least-squares regression (PLSR), reflectance spectroscopy.

- Plant ecologists use functional traits to describe how plants respond to and influence their environment. Reflectance spectroscopy can provide rapid, non-destructive estimates of leaf traits, but it remains unclear whether general trait-spectra models can yield accurate estimates across functional groups and ecosystems.
- We measured leaf spectra and 22 structural and chemical traits for nearly 2000 samples from 103 species. These samples span a large share of known trait variation and represent several functional groups and ecosystems, mainly in eastern Canada. We used partial least-squares regression (PLSR) to build empirical models for estimating traits from spectra.
- Within the dataset, our PLSR models predicted traits such as leaf mass per area (LMA) and leaf dry matter content (LDMC) with high accuracy ( $R^2 > 0.85$ ; %RMSE < 10). Models for most chemical traits, including pigments, carbon fractions, and major nutrients, showed intermediate accuracy ( $R^2 = 0.55–0.85$ ; %RMSE = 12.7–19.1). Micronutrients such as Cu and Fe showed the poorest accuracy. In validation on external datasets, models for traits such as LMA and LDMC performed relatively well, while carbon fractions showed steep declines in accuracy.
- We provide models that produce fast, reliable estimates of several functional traits from leaf spectra. Our results reinforce the potential uses of spectroscopy in monitoring plant function around the world.

## Introduction

Plant functional ecology relies on the measurement of traits that influence how plants interact with their abiotic and biotic environment. Such traits can be used to interpret or predict outcomes at the community scale or ecosystem scale (Funk *et al.*, 2017), ranging from species sorting across environmental gradients (Kunstler *et al.*, 2016) to rates of carbon and nutrient cycling (Cornwell *et al.*, 2008; Ollinger *et al.*, 2008). During the last 20 yr, ecologists have developed standardized trait protocols and databases to enable broad comparisons of plant functional strategies across species (Pérez-Harguindeguy *et al.*, 2013; Kattge *et al.*, 2020). Nevertheless, because trait measurement campaigns can be costly and challenging, trait databases remain sparse and much of the world's plant diversity is poorly represented (Kattge *et al.*, 2020). The resources needed to carry out intensive trait measurement campaigns using conventional methods have motivated the search for other approaches that could yield fast, reliable trait estimates.

One such approach is to predict plant traits from reflectance spectra, which report the fraction of light reflected from a surface across a range of wavelengths. For vegetation, the range most often studied is *c.* 350–2500 nm, which includes > 97% of solar radiation (American Society for Testing and Materials, 2020). Because the structure and chemistry of plant tissues determine their optical properties, many traits can be estimated from reflectance spectra measured at leaf or canopy scales (Jacquemoud & Ustin, 2019). At the leaf level, linking reflectance spectra and functional traits provides a fast way to estimate large numbers of leaf traits from individual plants. At the canopy level, it enables researchers to map traits using remote sensing, which may enable monitoring of plant community structure (Durán *et al.*, 2019; Zheng *et al.*, 2021) or biogeochemical cycles (Wessman *et al.*, 1988; Chadwick & Asner, 2018) over entire landscapes. Understanding leaf spectral variation is essential for scaling up to the canopy level (Asner *et al.*, 2011), and leaf-level spectral estimates of traits are part of many workflows for canopy trait mapping (Singh *et al.*, 2015; Wang *et al.*, 2020). These uses of

leaf spectra make it important to understand their functional drivers (Kothari & Schweiger, 2022).

Methods to predict traits from leaf or canopy spectra can be summarized into three groups: (1) simple indices calculated from reflectance at a few wavelength bands (e.g. Sims & Gamon, 2002); (2) physics-based radiative transfer models (RTMs; Jacquemoud *et al.*, 2009; Féret *et al.*, 2017); and (3) multivariate empirical methods that use large portions of the spectrum to build trait prediction models. Among this last group of methods, the most common is partial least-squares regression (PLSR), although others used include stepwise regression (Grossman *et al.*, 1996) and (more recently) machine learning approaches such as support vector machines and convolutional neural networks (Féret *et al.*, 2019; Pullanagari *et al.*, 2021). These methods are less mechanistic but offer the flexibility often needed to predict traits associated with complex optical properties (Curran, 1989). For example, predicting leaf nitrogen concentrations using RTMs has been a persistent challenge because leaves contain nitrogen in many forms, including proteins (e.g. RuBisCO) and pigments (Wang *et al.*, 2018; Féret *et al.*, 2021). Moreover, the absorption features of nitrogen-containing bonds often overlap with others, especially after being broadened by multiple scattering (Curran, 1989). As a result, leaf nitrogen is not identifiable with unique, distinct absorption features, and is often best predicted using empirical approaches like PLSR (Wang *et al.*, 2021). Researchers have likewise built PLSR models to estimate a wide variety of foliar traits from fresh-leaf spectra, including pigments (Yang *et al.*, 2016), non-structural carbohydrates (Ely *et al.*, 2019), condensed tannins (Couture *et al.*, 2016), and even more complex attributes such as leaf age (Chavana-Bryant *et al.*, 2017) and photosynthetic capacity (Yan *et al.*, 2021).

Estimating traits from leaf spectra has several advantages that may compensate for the sparsity of trait datasets. Compared to measuring a large number of traits, measuring spectra is fast, has low marginal cost, can be non-destructive, and requires less training. But since PLSR is purely empirical rather than mechanistic, a model calibrated using one dataset may yield inaccurate or biased predictions on another dataset if the association between traits and optical properties varies among contexts (Yang *et al.*, 2016; Wang *et al.*, 2020). The problem may be most severe when the model relies on absorption features that are not causally associated with the target trait, but rather with other covarying traits ('constellation effects' sensu Chadwick & Asner, 2016; Nunes *et al.*, 2017). This situation may occur most often when the target trait lacks major, well-defined absorption features, like concentrations of many elements (Nunes *et al.*, 2017). If trait covariance patterns vary among datasets, overfitting to the training data could cause such models to produce inaccurate trait estimates from new spectral data (Kothari & Schweiger, 2022). Empirical models may be especially fallible beyond the range of data used to train them (Schweiger, 2020; Burnett *et al.*, 2021).

To enable the widespread use of spectral models for trait prediction, it is essential to build general models that encompass the broadest possible range of spectral and trait diversity (Serbin *et al.*, 2019; Wang *et al.*, 2020). Such models could allow researchers to estimate plant traits from spectra in their study

systems without going through the laborious process of building their own models. Asner *et al.* (2011) invoked this goal in developing spectral models for many leaf traits in humid tropical forest canopies around the world. By contrast, Serbin *et al.* (2019) focused on a single trait (leaf mass per area; LMA) but included several functional groups and biomes from the tropics to the tundra. We sought to push this goal further by including both a large number of leaf traits and a broad range of ecosystems and functional groups, allowing us to compare which traits are the most practical targets for estimation by general spectral models.

We compiled foliar traits and spectra measured using standardized protocols on nearly 2000 samples that include trees, shrubs, graminoids, and other herbs from a range of ecosystems, mainly in eastern Canada (Table 1). We included structural and biochemical traits that relate to several aspects of leaf function, including nutrient economics, water relations, photosynthesis and photoprotection, and structural defense. We focused on building models to predict these traits from reflectance spectra, but we also compared the performance of reflectance, transmittance, and absorptance spectra. Among these properties, reflectance is the simplest and most common to measure because it bears the most relevance for interpreting remotely sensed canopy reflectance and does not require an integrating sphere. But since the content of leaf chemical constituents most directly alters the amount of light absorbed (Jacquemoud & Ustin, 2019), we conjectured that absorptance spectra might be better for estimating traits, and aimed to determine whether any potential benefit transmittance or absorptance spectra provide in trait estimation outweighs their greater costs in time and equipment.

The performance of statistical models is often evaluated by splitting a dataset at random into calibration and validation subsets. This procedure represents a best-case scenario, since the data are all collected with the same protocols and, based on the mathematics of random sampling, the two subsets must have similar distributions of predictor and response variables. Therefore, we validated our models on both a random subset of our dataset (internal validation) and on independent datasets (external validation) – the latter perhaps representing a more realistic test of how they would perform in practical applications.

Concerns about the generality of spectral trait models also raise the question: What factors determine whether a trait model yields accurate predictions on an external dataset? Many existing models to predict leaf traits were built using samples belonging to a single functional group or ecosystem, leaving it an open question how they would transfer to new settings. One might expect that models would show poorer performance as the calibration samples (used to build the model) and the external dataset's samples become less functionally similar (Yang *et al.*, 2016). But if the models show consistently strong performance, it would suggest that associations between traits and optical properties are robust, not contingent on the particular samples included. To examine model transferability, we divided our dataset by functional group and examined model accuracy using each functional group in turn as the validation dataset for models calibrated using the remaining functional groups. We posed two hypotheses about

**Table 1** A summary of all projects with samples included in the study.

Project	Description	Latitude range	Longitude range	Species	Samples per functional group							Total
					Broadleaf	Conifer	Graminoid	Fern	Forb	Shrub	Vine	
Beauchamp-Rioux	Nine common broadleaf tree species measured from June to October 2018 at multiple forested sites in Québec (Beauchamp-Rioux, 2022)	45°24'–45°59'N	73°19'–75°31'W	9	436							436
Blanchard	A sampling of nearly all tree species found in southern Québec, collected across multiple sites throughout summer 2019	45°6'–46°N	73°19'–74°4'W	43	270	68				3		341
Boucherville 2018	A variety of plants sampled in August 2018 from the Parc national des Îles-de-Boucherville in southern Québec	45°38'N	73°28'W	12			14		30	22	6	72
Boucherville 2019	A variety of plants sampled in July 2019 from the Parc national des Îles-de-Boucherville in southern Québec	45°38'N	73°28'W	19	40		38		59	26	10	173
CABO General	A small number of samples from southern Québec not collected as part of a specific project	45°28'–45°59'N	71°52'–74°4'W	13	33		6		3	39		81
Crofts	Trees sampled in July 2019 across an altitudinal gradient in southeastern Québec, along the transition from temperate deciduous to boreal forest	45°25'–45°29'N	71°7'–71°13'W	24	139	60				5		204
Girard	Four common bog plants sampled in summer 2018 in Ontario and southern Québec across a gradient of nitrogen deposition (Girard <i>et al.</i> , 2020)	45°25'–46°46'N	71°4'–75°32'W	4			23			72		95
Hacker	Plants sampled in May 2019 to evaluate functional trait variation throughout an endangered oak savannah in British Columbia (Hacker <i>et al.</i> , 2022)	48°47'–48°49'N	123°38'–123°39'W	23	10		38	7	90	56		201
<i>Phragmites</i> temporal	Five co-occurring wetland plant species sampled from June to September 2019 in Boucherville, Québec (Pardo, 2021)	45°35'–45°39'N	73°27'–73°29'W	5			240		60			300
Warren	<i>Agonis flexuosa</i> sampled in November 2018 along a chronosequence of increasing soil age in southwestern Australia (Turner <i>et al.</i> , 2018)	34°36'–34°49'S	115°52'–116°4'E	1	68							68
Total				103	996	128	359	7	242	223	16	1971

CABO, Canadian Airborne Biodiversity Observatory.

these analyses: (1) For a given trait, predictions are most accurate when the trait distributions are most similar between the calibration and validation datasets; and (2) traits whose predictions are most accurate on random subsets of the full dataset will also yield the most accurate predictions (on average) when transferring models onto left-out functional groups. We aimed to shed light on the factors that influence a model's accuracy across a range of settings.

## Materials and Methods

### Sampling

We assembled a database ( $n = 1971$ ; species = 103) of leaf spectra and functional traits measured as part of the Canadian Airborne Biodiversity Observatory (CABO; [www.caboscience.org](http://www.caboscience.org)). We aggregated data from 10 individual projects carried out during 2018 and 2019 at sites across temperate Canada and one site in southwestern Australia (Table 1). The sites span a wide range of edaphic properties, from nutrient-poor bogs and phosphorus-limited woodlands to

highly fertile post-agricultural and wetland sites. Each sample comprised a large, homogeneous group of sunlit leaves, which we divided up for spectral and trait measurements. We classified samples into seven functional groups: broadleaf trees, coniferous trees, ferns, forbs, graminoids, shrubs, and vines (Table 1). Further details on sampling protocols and functional groups are found in Supporting Information Methods S1.

### Leaf spectral and trait measurements

We measured directional-hemispherical reflectance and transmittance spectra (350–2500 nm) using an HR-1024i spectroradiometer equipped with a DC-R/T integrating sphere from Spectra Vista Corp. (Poughkeepsie, NY, USA). For each sample, we measured spectra from the adaxial surface of six leaves or (for small or narrow leaves) leaf arrays. We resampled spectra to 1 nm resolution, averaged spectra from the same sample, and trimmed them to 400–2400 nm by removing the ends, which are often noisy. Finally, we calculated absorptance at each wavelength by subtracting the sum of reflectance and transmittance from 1.

Further details on spectral measurement and processing can be found in Methods S1.

We measured the following traits on each leaf sample: leaf mass per area (LMA), leaf dry matter content (LDMC), equivalent water thickness (EWT; defined as foliar water volume per area), and concentrations of soluble cell components, hemicellulose, cellulose, lignin, Chl *a*, Chl *b*, total carotenoids, and a number of elements (Al, C, Ca, Cu, Fe, K, Mg, Mn, N, Na, P, and Zn). Elements other than C and N were only available for a few projects that account for about one-third ( $n = 678$ ) of the total samples. Further details on trait measurement protocols can be found in Methods S1. We compared our trait distributions to the TRY trait database to evaluate how well they span the global range of trait variation. Although it has known geographic and taxonomic biases, TRY is the most comprehensive database of its kind (Kattge *et al.*, 2020). We also performed a principal components analysis (PCA) on the scaled and centered trait data to visualize patterns of trait variation among our samples.

Within a dataset, chemical traits may vary more in proportion to the mass or the area of the leaf (Osnas *et al.*, 2013). When a trait is distributed mainly proportional to leaf area, mass-normalization induces a negative correlation with LMA. Since interspecific variation in pigments tends to be area proportional, Kattenborn *et al.* (2019) used this principle, among others, to argue that pigment content (per unit area) is a better target than concentration (per unit mass) for remote sensing-based estimation. We applied our PLSR modeling approach to both mass- and area-based traits, but we focus on mass-based models because conventional protocols measure most chemical traits on a mass basis, and because most of our chemical traits were more mass proportional. Chemical traits should be assumed here to be mass-based when left unspecified. We calculated the mass proportionality of each chemical trait in our dataset as the ordinary least squares slope between the  $\log_{10}$ -transformed area-normalized trait and  $\log_{10}$ -transformed LMA (Osnas *et al.*, 2013).

## PLSR modeling

**Trait estimation** Due to the high dimensionality and multicollinearity of spectral data, we used a PLSR modeling approach to build trait estimation models. PLSR projects the high-dimensional input dataset (here, spectra) onto a smaller number of latent components constructed to maximize their covariance with the variable(s) to be predicted (traits). We built separate models using reflectance, transmittance, and absorbance as predictors, in each case using the whole trimmed spectrum (400–2400 nm). We did not transform the distributions of any trait to reduce skewness, as is sometimes recommended (Burnett *et al.*, 2021); in preliminary tests, such transformations did not yield clear, consistent improvements in model performance (Fig. S1). We performed all analyses in R v.3.6.3 (R Core Team, 2020).

We calibrated and validated our main set of models ('primary models') largely following the example of Serbin *et al.* (2014) and Burnett *et al.* (2021) using R package *PLS* v.2.7.1 (Mevik *et al.*, 2019). First, we divided the full dataset into 75%

calibration and 25% validation sets at random, stratified by the functional group (Table 1). We fit a preliminary PLSR model for each trait on the calibration subset and used 10-fold cross-validation to select the number of components to use in our final models. We chose the smallest number of components that brought the cross-validation root mean squared error of prediction (RMSEP) within one SE of the global minimum – a distinct number (4–27) for each trait and type of spectrum. We calculated the variable influence on projection (VIP) metric (Wold *et al.*, 2001) to determine which spectral regions were most important for predicting each trait.

Next, we fit our final models through a jackknife resampling procedure in which we further divided the 75% calibration dataset 100 times into random 70% training and 30% testing subsets. For each iteration, we built a model from the 70% training dataset using the previously chosen number of components and applied it to the 30% testing dataset. This procedure allowed us to get a distribution of summary statistics that shows how model performance varies based on random changes in the training and testing datasets. The primary model comprises the ensemble of 100 sets of coefficients for each trait – one derived from each iteration of the 70%/30% split – which we applied to the 25% validation dataset to get a distribution of estimates for each sample. We call this procedure an 'internal validation' because the calibration and validation datasets were divided at random from the same set of samples. We compared the measured values to the mean estimates for each trait to produce summary statistics ( $R^2$ , RMSE, %RMSE). For robustness to outliers, we defined %RMSE as the RMSE divided by the range of the inner 95% of trait values, in contrast to a more common definition (Burnett *et al.*, 2021) that uses the full range.

**External validation** We compiled data from three sources as external validation datasets for our primary models. The first two are LOPEX (Hosgood *et al.*, 1994) and ANGERS (Féret *et al.*, 2008), which have been widely used to validate methods for plant trait estimation from reflectance spectra. Between them, these datasets include > 500 samples and several dozen species of temperate (mostly European) broadleaf trees, shrubs, herbs, and vines – many of them agricultural or ornamental. The third source is an expanded version of the Dessain dataset previously described in Kothari *et al.* (2023), which mainly includes sunlit broadleaf trees, shrubs, and herbs from southern Québec and has a large overlap in species with the CABO data. Unlike LOPEX and ANGERS, most of the Dessain trait data were measured using the same protocols as the core CABO datasets. All three datasets were measured using integrating spheres and include similar spectral ranges, but the instruments and their specifications differ from each other and the core datasets we used to train the models, which can cause slight but important differences in measured reflectance (Lukeš *et al.*, 2017; Hovi *et al.*, 2018).

We used these datasets to externally validate only our reflectance-based models because we did not have transmittance and absorbance spectra for the Dessain project. We applied our sets of reflectance-based coefficients from resampling analyses (100× for each trait) to the spectra in each dataset and took the



mean of the resulting 100 estimates for each sample for comparison to the measured traits. Not all traits were available for each dataset. Further details on our handling of external validation data are in Methods S2.

**Model transferability among functional groups** Besides assessing the viability of our primary models, we also aimed to test whether and when models could estimate traits accurately on a group of species functionally distinct from those used in calibration (Hypotheses 1 and 2). To this end, we built another set of models: we selected a single functional group at a time as a validation dataset and used the reflectance spectra of the remaining functional groups to calibrate a PLSR model for each trait. We performed 10-fold cross-validation and component selection as described earlier, but omitted the jackknife procedure. Finally, we applied the model to the validation functional group. We repeated this procedure using each functional group in turn as the validation dataset, besides ferns and vines because of their low numbers of samples. Among elements, we only considered C and N because other elements were only available for certain projects and we could not guarantee adequate coverage of all functional groups. We quantified performance using  $R^2$ , RMSE, and %RMSE – calculating %RMSE using the inner 95% trait range of the full dataset in the denominator rather than the inner 95% trait range of only the validation functional group. This metric, which we call %RMSE<sub>full</sub> to reduce ambiguity, avoids apparent reductions in model performance due to a narrow trait range in the validation functional group.

We conjectured that for a given trait, model performance would decline as the calibration and validation datasets became more dissimilar in their trait distributions (Hypothesis 1). We quantified dissimilarity using the Hellinger distance between the calibration and validation datasets' distributions for each trait, as estimated in R package STATIP v.0.2.3 (Poncet & R Core Team, 2019). Here we focused on %RMSE<sub>full</sub> because it is normalized to the scale of the data (unlike RMSE) and incorporates bias (unlike  $R^2$ ). We tested the influence of trait dissimilarity on %RMSE<sub>full</sub> with analysis of covariance (ANCOVA) using the Hellinger distance (continuous), the trait identity (categorical), and their interaction as predictors.

## Results

### Trait and spectral variability

The ranges for most traits in our dataset spanned most of the trait ranges in TRY. Many traits, including LMA, EWT, and all elements other than C and N, had distributions with strong positive skew in both TRY and CABO data, resulting in a long upper tail of high values (Fig. 1). For certain elements (Al, Cu, Fe, K, Mg), the CABO dataset had less representation of values along the upper tail than TRY. For other elements (Na, P, Zn), as well as LDMC, N, and pigments, the CABO data had greater representation of high values. For yet other traits (LMA and C), the CABO data had a somewhat narrower range toward either extreme.

Within the dataset, functional groups often differed in their trait values, as shown by a principal components analysis (PCA) of the centered and scaled trait data (excluding elements other than C and N; Fig. S2). The first two PCs of the trait data explained 65.7% of total variance. Graminoids were distinguished by high concentrations of hemicellulose and cellulose and low concentrations of soluble carbon, lignin, and total C. Leaf mass per area and LDMC were negatively correlated with N and pigment concentrations; conifers (besides deciduous *Larix laricina* (Du Roi) K. Koch) and the evergreen broadleaf tree *Agonis flexuosa* (Willd.) Sweet had particularly high LMA and LDMC, while other functional groups each contained significant variation along this axis. High values of EWT (> 0.3 mm) were dominated by evergreen conifers and graminoids adapted to wetlands, such as *Typha angustifolia* L. and *Phragmites australis* (Cav.) Trin. ex Steud. *Agonis flexuosa* represented most of the samples with the lowest concentrations of P, K, and Fe and the highest concentrations of Na, while bog shrubs and sedges had particularly low Ca concentrations. The large fraction of variance explained by major trait axes indicates that certain clusters of traits covary strongly, often in ways that correspond to functional groups.

Our samples showed the typical shape of leaf spectra, including a sharp increase in reflectance and transmittance ('red edge') between the visible and near-infrared (NIR; 700–1000 nm) ranges and prominent water absorption bands in the short-wave infrared (SWIR; > 1000 nm) range (Figs 2, S3). Compared with other functional groups, needleleaf conifers had low reflectance and transmittance and high absorptance across the spectrum. Forbs also tended to have lower transmittance and higher absorptance in the SWIR. In absolute terms, absorptance and transmittance spectra had greater variation than reflectance spectra, especially in the SWIR.

### PLSR modeling

**Internal calibration and validation** The accuracy of trait estimates from reflectance spectra varied widely by trait (Table 2; Figs 3, 4, S4–S10). Our primary models estimated structural and water-related traits – LMA ( $R^2 = 0.892$ ; %RMSE = 8.04), EWT ( $R^2 = 0.885$ ; %RMSE = 8.46), and LDMC ( $R^2 = 0.867$ ; %RMSE = 9.78) – with high accuracy. Models for certain chemical traits such as carbon fractions ( $R^2 = 0.558$ – $0.826$ ; %RMSE = 12.7–19.1), major elements such as C, N, K, and Ca ( $R^2 = 0.541$ – $0.747$ ; %RMSE = 13.2–20.4), and pigments ( $R^2 = 0.644$ – $0.689$ ; %RMSE = 13.8–15.0) also showed intermediate-to-high accuracy. Finally, models for some micronutrients like Cu ( $R^2 = 0.295$ ; %RMSE = 25.9) or Mn ( $R^2 = 0.254$ ; %RMSE = 22.8) performed very poorly. For pigments, N, and some other elements, models underestimated trait values at the sparsely represented upper tail of the measured range, while for C the models overestimated values at the sparse lower tail (Figs 3, 4). Trait models with lower accuracy in internal validation also had greater variability in accuracy across iterations in the resampling analysis – even when leaving out elements other than C and N, which also had fewer samples (Figs S11–S13).

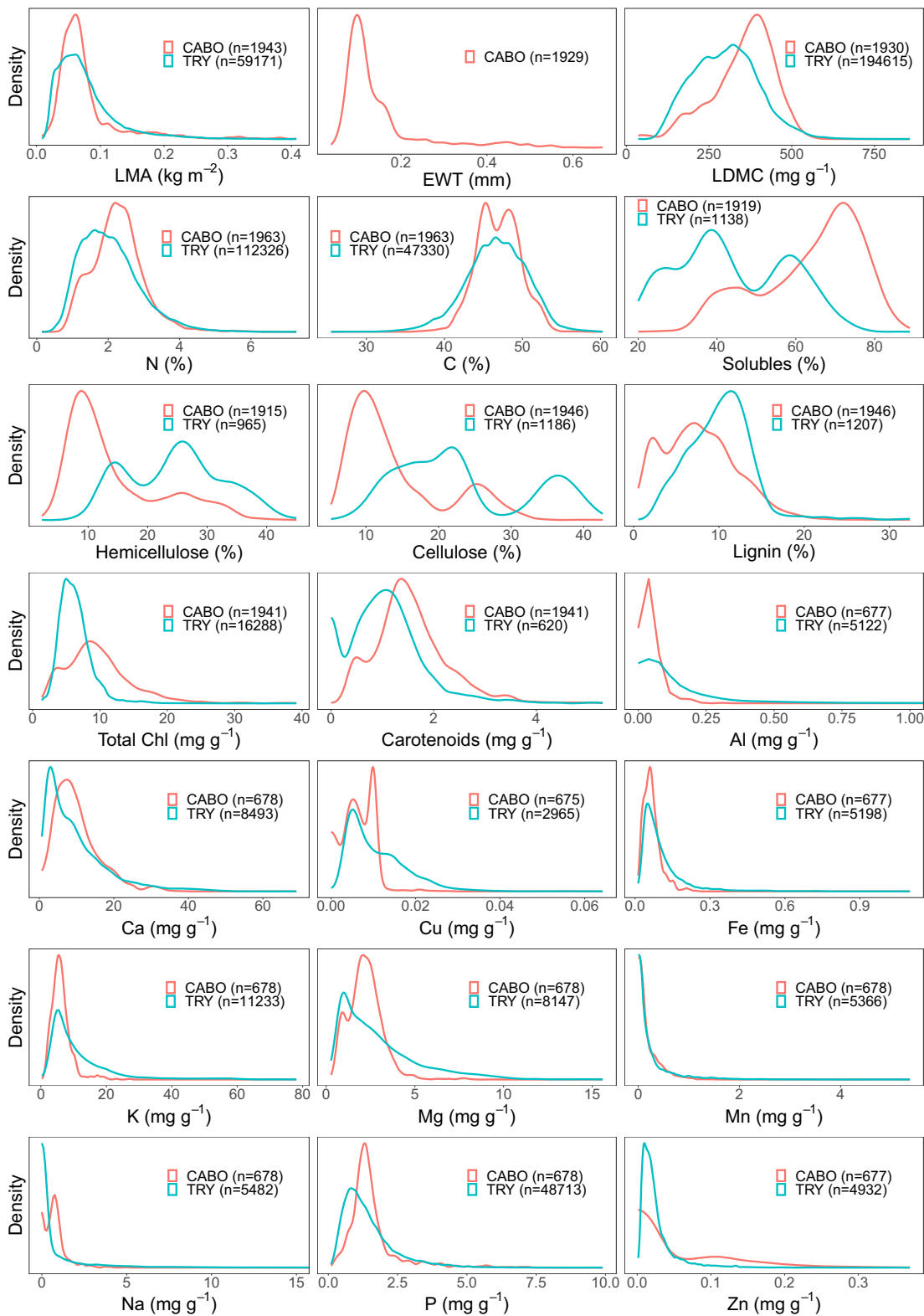


**Fig. 1** Density plots comparing the distributions of various leaf structural and chemical traits in the Canadian Airborne Biodiversity Observatory (CABO) dataset to the TRY database (Kattge *et al.*, 2020). We filtered TRY data to include only values with an error risk below 3. Equivalent water thickness (EWT) is only shown for CABO because it is not a trait in TRY. Elements besides C and N are only available for the Beauchamp-Rioux, Boucherville 2018, Girard, and Warren projects. LDMC, leaf dry matter content; LMA, leaf mass per area.

The VIP metric revealed broad similarities in the regions of the spectrum that were important for predicting different traits from reflectance spectra (Figs S14–S16). In particular, major features of the visible region, including the green hump (centered at 550–560 nm) and especially the inflection point of the red edge (710–720 nm), were important for predicting most traits besides

EWT. These visible-range importance peaks (especially at the red edge) were often higher for traits such as Al, Zn, Mn, and hemicellulose than for pigments, which are the dominant drivers of visible reflectance (Jacquemoud & Ustin, 2019). In general, VIP declined into the NIR but had several peaks in the SWIR, including relatively distinct peaks for multiple traits at 1390 and 1880 nm, and weaker ones at 1720, 2020, 2150, and 2290 nm. For EWT, LMA, Cu, Fe, and Na, VIP remained high throughout a larger portion of the SWIR; uniquely, EWT had its global maximum VIP at 1390 nm.

In the dataset, most chemical traits were distributed mainly proportional to mass (Table S1). Exceptions included all pigments and several macronutrients and micronutrients, which showed mass proportionality <0.5. We produced estimates of area-based chemical traits both by building models to estimate them directly and by multiplying estimated mass-based traits by estimated LMA (Table S1; Figs S17–S20). For most traits, estimating area-based traits directly yielded more accurate estimates; the difference was greatest for pigments, Ca, Cu, N, P, which all have area proportionality <0.6. However, multiplying mass-based estimates by LMA estimates was slightly more accurate for many highly mass-proportional traits, including Al, C, Na, and cellulose.

For most traits, transmittance and absorbance spectra yielded slight improvements in performance relative to reflectance (Table S2; Figs S4–S13). Excluding traits that showed very poor

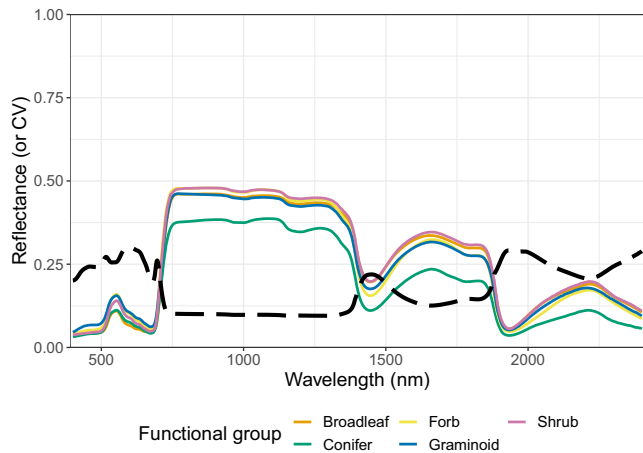


**Fig. 2** The median leaf reflectance at each wavelength across the spectrum, separated by functional group. We omit ferns and vines, which are only represented by one species each. The dashed line shows the coefficient of variation across all samples.

**Table 2** Summary statistics for the performance of reflectance-based models calibrated on CABO data and applied to internal and external validation datasets.

	Internal					Dessain			LOPEX			ANGERS		
	No. obs	No. comps	R <sup>2</sup>	RMSE	%RMSE	R <sup>2</sup>	RMSE	%RMSE	R <sup>2</sup>	RMSE	%RMSE	R <sup>2</sup>	RMSE	%RMSE
LMA (kg m <sup>-2</sup> )	1943	23	0.892	0.0175	8.04	0.593	0.0855	123	0.657	0.111	112	0.519	0.137	117
LDMC (mg g <sup>-1</sup> )	1930	20	0.867	32.9	9.78	0.824	40.6	13.6	0.860	46.4	12.0			
EWT (mm)	1929	13	0.885	0.0334	8.46	0.629	0.0395	24.2	0.888	0.0705	27.5	0.825	0.0665	34.8
N (%)	1963	19	0.709	0.403	13.7	0.417	0.664	21.6	0.537	0.854	20.2			
C (%)	1963	20	0.747	1.38	13.2	0.410	2.23	31.6	0.148	2.81	25.5			
Solubles (%)	1919	23	0.733	6.59	15.1	0.284	10.9	26.7						
Hemicellulose (%)	1915	20	0.695	4.35	16.1	0.324	5.28	19.7						
Cellulose (%)	1946	25	0.826	2.74	12.7	0.327	6.68	43.5	0.355	5.47	23.1			
Lignin (%)	1946	20	0.558	2.82	19.1	0.152	4.68	29.9	0.167	4.79	26.8			
Chla (mg g <sup>-1</sup> )	1941	13	0.689	2.07	13.8	0.312	2.88	26.7	0.411	2.72	28.1	0.505	2.80	21.9
Chlb (mg g <sup>-1</sup> )	1941	14	0.679	0.716	15.0	0.318	1.05	31.6	0.443	0.927	23.4	0.412	1.32	28.7
Carotenoids (mg g <sup>-1</sup> )	1941	12	0.644	0.434	14.7	0.195	0.585	27.0	0.290	0.694	24.8	0.421	1.09	29.9
Al (mg g <sup>-1</sup> )	677	6	0.304	0.0293	24.6	0.006	0.0813	33.5						
Ca (mg g <sup>-1</sup> )	678	17	0.541	4.03	20.4	0.009	10.4	32.8						
Cu (mg g <sup>-1</sup> )	675	5	0.295	0.00311	25.9	0.004	0.0147	34.0						
Fe (mg g <sup>-1</sup> )	677	4	0.286	0.0295	23.0	0.045	0.053	26.6						
K (mg g <sup>-1</sup> )	678	10	0.550	2.32	15.7	0.443	9.13	28.9						
Mg (mg g <sup>-1</sup> )	678	18	0.394	0.714	22.8	0.149	2.3	53.6						
Mn (mg g <sup>-1</sup> )	678	10	0.254	0.164	22.8	0.005	0.504	54.6						
Na (mg g <sup>-1</sup> )	678	6	0.519	0.451	16.7	0.085	0.881	22.6						
P (mg g <sup>-1</sup> )	678	15	0.313	0.607	20.5	0.051	2.06	51.2						
Zn (mg g <sup>-1</sup> )	677	17	0.487	0.0486	24.2	0.045	0.118	34.9						

%RMSE is calculated as RMSE divided by the inner 95% trait range. The column 'No. obs' refers to the number of observations for the trait in the full CABO dataset. The column 'No. comps' refers to the number of PLSR components selected. CABO, Canadian Airborne Biodiversity Observatory; EWT, equivalent water thickness; LDMC, leaf dry matter content; LMA, leaf mass per area; RMSE, root mean squared error.

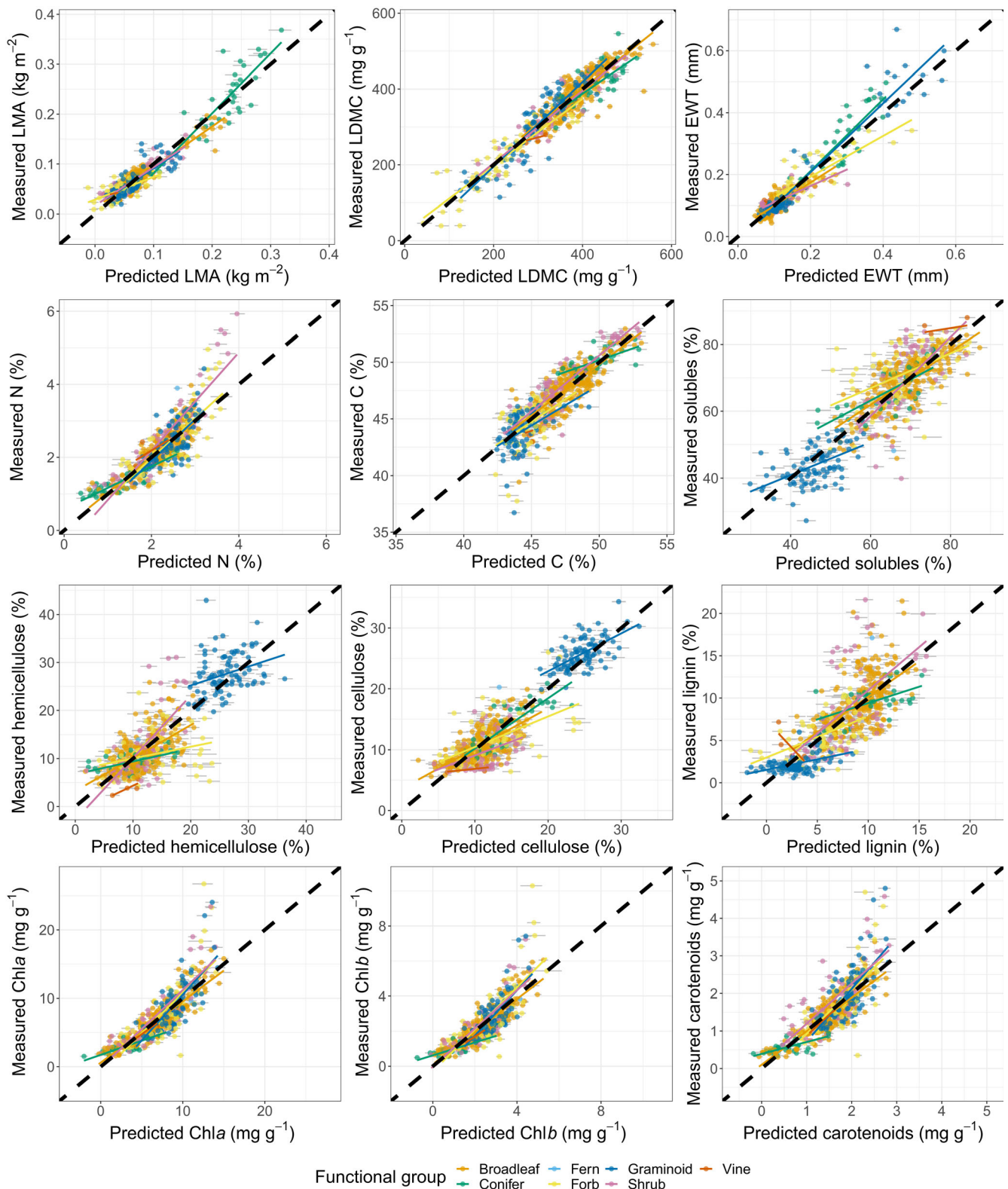


**Fig. 3** Plots of observations against reflectance-based partial least-squares regression predictions among internal validation data for various leaf structural and chemical traits. The black dashed line in each panel is the 1 : 1 line. Colored lines represent best-fit lines from ordinary least squares (OLS) regression for each functional group. Error bars around each point represent 95% confidence intervals based on the ensemble of models produced in the 100× jack-knife analysis. EWT, equivalent water thickness; LDMC, leaf dry matter content; LMA, leaf mass per area.



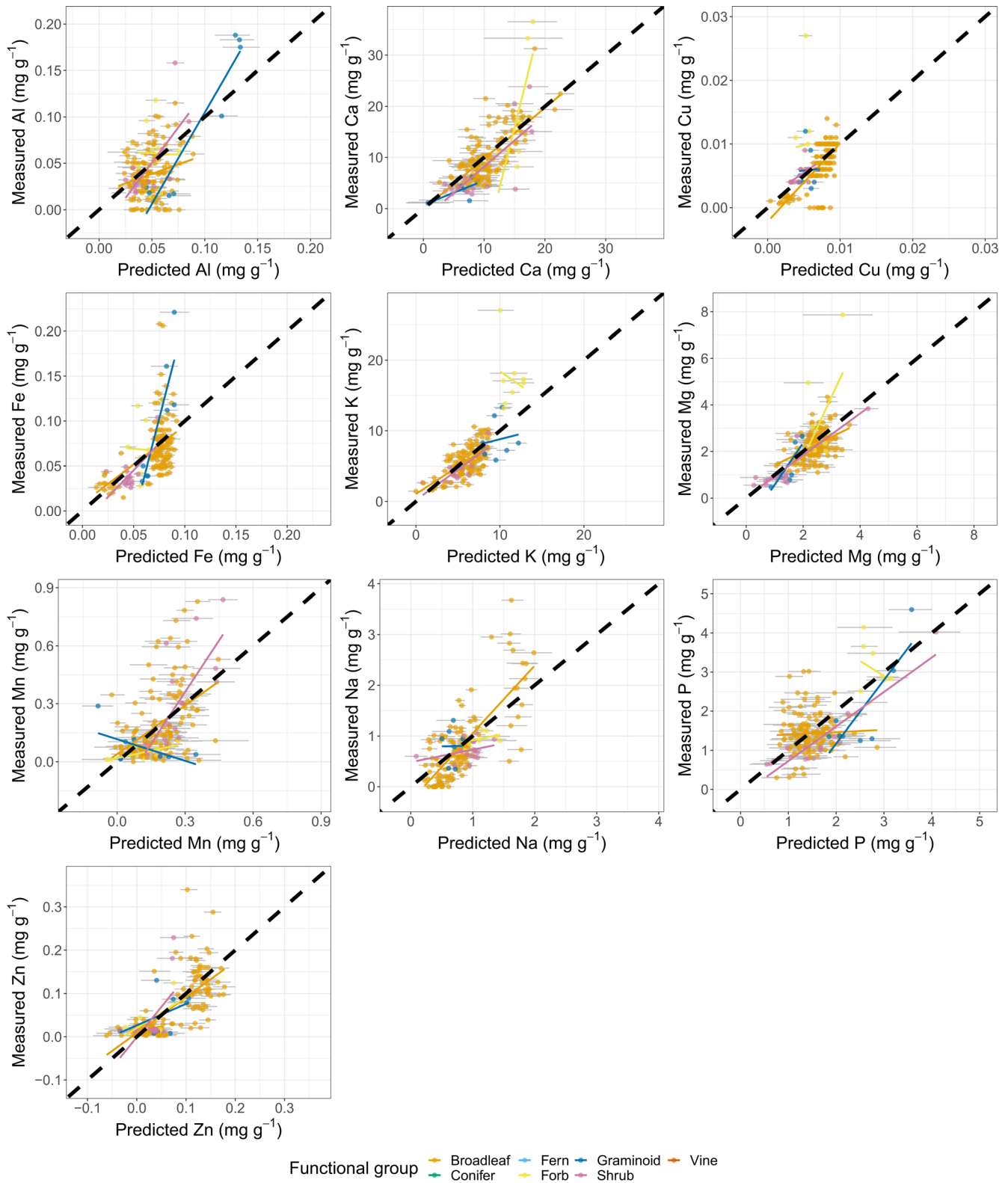


**Fig. 4** Plots of observations against reflectance-based partial least-squares regression predictions among internal validation data for elements other than C and N. These data are only available for the Beauchamp-Rioux, Boucherville 2018, Girard, and Warren projects. The black dashed line in each panel is the 1 : 1 line. Colored lines represent best-fit lines from ordinary least squares (OLS) regression for each functional group. Error bars around each point represent 95% confidence intervals based on the ensemble of models produced in the 100× jackknife analysis.

performance in general (average  $R^2 < 0.35$ ), the greatest improvements between reflectance and either transmittance or absorbance spectra (average  $\Delta\%RMSE > 1$ ) occurred for LMA, LDMC, EWT, pigments, Ca, K, N, and P. Using transmittance or absorbance spectra never worsened performance considerably (average  $\Delta\%RMSE < -1$ ).

**External validation** We applied our reflectance-based primary models for each trait to three external validation datasets whose spectral and trait measurement protocols differed from the CABO dataset. In general, models performed less well on these independent datasets than the internal validation (Tables 2, S3, S4; Figs 5, 6, S21). The traits that had the highest  $R^2$  between observed and predicted values in the internal validation also had the highest  $R^2$  in the external validation. As a result, structural and water-related traits (LMA, LDMC, and EWT) had moderate-to-high  $R^2$  in the external validation (0.590–0.842 averaged across datasets). The RMSE for LDMC predictions was only slightly higher than in the internal validation (40.6–46.4 vs 32.9 mg g<sup>-1</sup>). By contrast, both LMA and EWT were greatly overestimated for most samples, so even though the  $R^2$  was moderate-to-high, RMSE was also high (LMA: 0.0855–0.137 vs 0.0175 kg m<sup>-2</sup>; EWT: 0.0395–0.0705 vs 0.0334 mm). Pigments, N, and particularly C and carbon fractions had correspondingly lower prediction accuracy and varying amounts of bias. Many other macro- and micronutrients (besides K) had very low prediction accuracy ( $R^2 < 0.15$ ).

**Model transferability among functional groups** For each trait, models generally performed worse when applied to a functional group left out from the calibration dataset than when (as in our primary models) calibrated and applied to random selections of samples (Figs 6, 7; Table S5). In particular, models calibrated using the other functional groups tended to show poor performance when applied to graminoids or forbs. Carbon fractions tended to be estimated with relatively low accuracy (high RMSE, low  $R^2$ ); because these carbon fractions were predicted well within the internal validation, this result weakened the relationship posited in Hypothesis 2 between average model performance in internal validation and in functional group transferability analyses. Models for carbon fractions applied to graminoids yielded particularly biased predictions, with %RMSE<sub>full</sub> > 50 for all but lignin. While graminoids were distinctively high in hemicellulose and cellulose and low in solubles and lignin, the model predicted them to be much more similar to the other functional groups (Fig. 7). Models for LMA applied to conifers likewise showed %RMSE<sub>full</sub> > 50 because the distinctively high values of evergreen (non-*Larix*) conifers were underestimated.

In our ANCOVA model, there were significant effects of trait ( $F_{11,36} = 2.626$ ;  $P = 0.014$ ), Hellinger distance ( $F_{1,36} = 21.066$ ;  $P < 10^{-4}$ ), and their interaction ( $F_{11,36} = 4.139$ ;  $P < 0.001$ ) on %RMSE<sub>full</sub>. This result led us to perform separate linear regressions between %RMSE<sub>full</sub> and Hellinger distance for each trait (Fig. 6b). The relationship was significant and positive for LMA ( $t(3) = 7.141$ ;  $P = 0.006$ ), but not significant and highly variable

in strength and direction among the other traits. Support for Hypothesis 1 was thus also weak and equivocal.

## Discussion

We built PLSR models to predict widely used foliar traits from reflectance spectra across nearly 2000 samples of 103 species, including several functional groups and ecosystems. Our findings underscore that leaf spectra integrate many aspects of leaf phenotypes in a single measurement (Cavender-Bares *et al.*, 2017; Kothari & Schweiger, 2022) and help explain why spectral variation can serve as a surrogate for phenotypic variation (Schweiger *et al.*, 2018; Frye *et al.*, 2021).

### Comparing PLSR model performance among traits

The performance of our primary models was highest for structural and water-related traits (LMA, LDMC, and EWT), corroborating studies that have reported high accuracy using diverse modeling approaches (Serbin *et al.*, 2019; Guzmán Q & Sanchez-Azofeifa, 2021). Indeed, the contents of dry matter and water are strong drivers of optical properties across much of the NIR and SWIR (Féret *et al.*, 2008). Our models predicted N, C, individual carbon fractions, and pigments with intermediate accuracy. These traits also have known influences on leaf optical properties. Pigments control optical properties in the visible range ( Jacquemoud & Ustin, 2019) and correlate with N. Cellulose, lignin, and N-containing compounds like proteins also have bonds with known (if weak) absorption features, primarily in the NIR and SWIR (Curran, 1989).

Models for elements at low concentrations often showed poor performance. Most of these elements have no measurable absorption features in this range, so their concentrations can only be estimated indirectly, often through symptoms of nutrient deficiency (Jacquemoud & Ustin, 2019). In some cases, our models could predict variation across, but not within, major biological groups. For example, Na could be predicted with  $R^2 = 0.519$ , but mainly because Australian *A. flexuosa* has on average more than twice the Na concentration of other species sampled. The model could have incorporated any optical features that distinguish *A. flexuosa* from other specimens, whether or not those features truly result from Na concentration. This kind of constellation effect may underlie the spectroscopic estimation of many elements (Nunes *et al.*, 2017; Kothari & Schweiger, 2022).

### Interpreting PLSR models

The VIP metric revealed strong similarities across traits in the major peaks of importance, including the green hump, the red edge, and multiple features in the SWIR (e.g. 1390 and 1880 nm; Figs S14–S16). The general pattern of high VIP along the green hump and at the red edge is shared by many traits across studies (Yang *et al.*, 2016; Ely *et al.*, 2019; Yan *et al.*, 2021; Kothari *et al.*, 2023). In general, visible and red edge reflectance are dominated by pigments and leaf structure (Richardson *et al.*, 2002). Many traits show isolated VIP peaks in

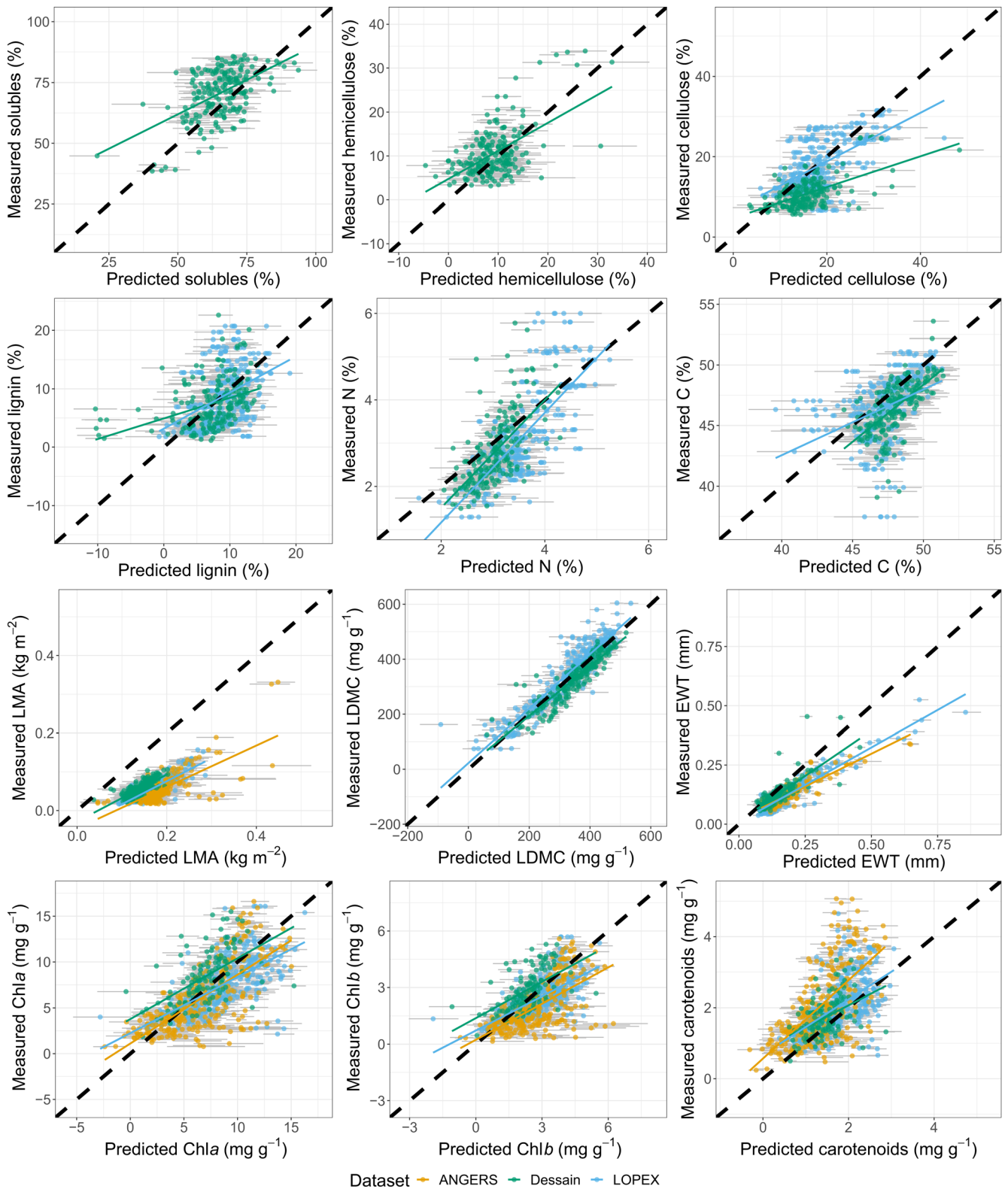


**Fig. 5** Plots of observations against reflectance-based partial least-squares regression predictions among external validation data for various leaf structural and chemical traits. The black dashed line is the 1 : 1 line. Colored lines represent best-fit lines from ordinary least squares (OLS) regression for each dataset. Error bars around each point represent 95% confidence intervals based on the ensemble of models produced in the 100× jackknife analysis. EWT, equivalent water thickness; LDMC, leaf dry matter content; LMA, leaf mass per area.

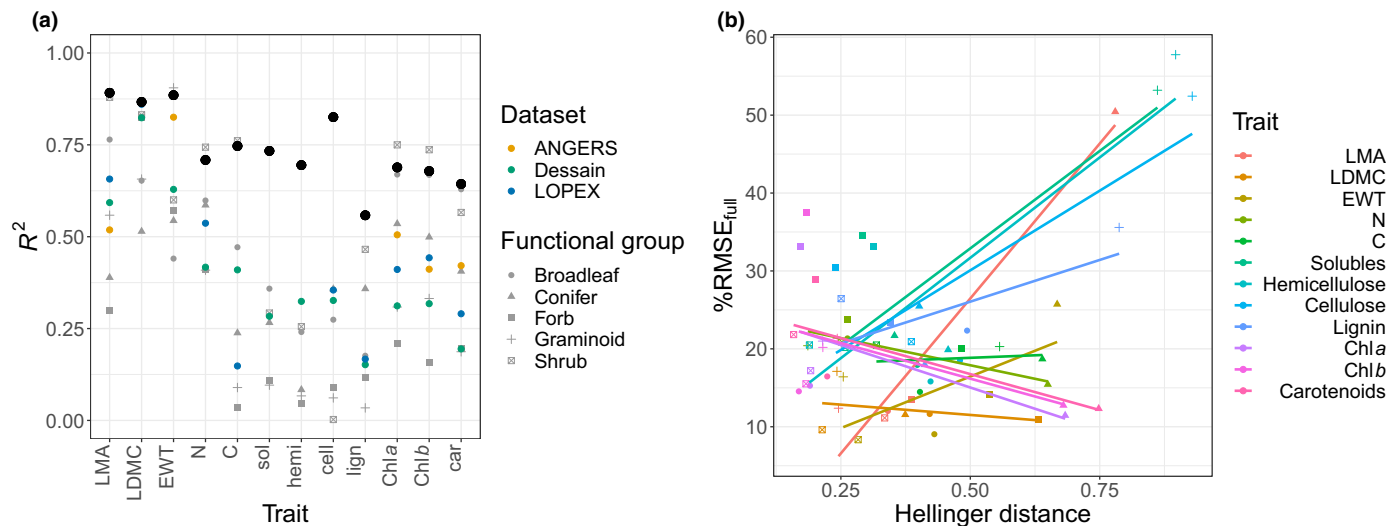


**Fig. 6** (a) A summary of model  $R^2$  for each trait. Colors indicate whether the  $R^2$  describes performance of models on: the randomly selected 25% internal validation dataset (black dots); specific functional groups used as validation data in model transferability analyses; or external validation datasets. (b) The relationship between %RMSE and the Hellinger distance between calibration and validation trait distributions in model transferability analyses. Functional group symbols are shared between panels and refer to the validation functional group. car, total carotenoids; cell, cellulose; EWT, equivalent water thickness; hemi, hemicellulose; LDMC, leaf dry matter content; lign, lignin; LMA, leaf mass per area; sol, solubles.

the SWIR, which are harder to explain in terms of specific traits. Two peaks are in off-center parts (1390 and 1880 nm) of major water absorption features, and the SWIR also contains many shallow, overlapping absorption features of bonds in dry matter components, making it hard to isolate the influence of any single one (Curran, 1989). In contrast to these distinct peaks, LMA and EWT (as well as some elements) had high VIP throughout much of the SWIR, which might arise from the strong and pervasive influence of LMA and EWT on SWIR reflectance.

Similarities in VIP may result from trait covariance (Fig. S2), which could allow models to leverage constellation effects. Some cases are clear: the three pigment pools correlate tightly with each other ( $R^2 = 0.853\text{--}0.974$ ) and with N ( $R^2 = 0.457\text{--}0.517$ ), and their VIP patterns share an overall visual similarity. Likewise, solubles, hemicellulose, and cellulose are closely linked ( $R^2 = 0.643\text{--}0.834$ ) and have similar VIP patterns. Other explanations are more elusive: for example, all four carbon fractions have high VIP across the green hump and red edge, but correlate poorly ( $R^2 = 0\text{--}0.107$ ) with pigments and LMA, which account for most spectral variation in those regions. Such findings imply that strong covariance with a few key traits cannot alone explain the striking similarities in VIP, nor the high accuracy of models for traits like carbon fractions in the internal validation.

### Alternate PLSR models

We focused on estimating chemical traits on a mass basis, but the remote sensing literature contains strong arguments for estimating certain constituents on an area basis. In particular, leaf optical properties are driven more by the absolute quantity of a constituent than its quantity relative to other constituents. This consideration should matter most for traits distributed in proportion to area (Kattenborn *et al.*, 2019). In our dataset, pigments and

several nutrients were mostly area proportional (Table S1). As Kattenborn *et al.* (2019) suggested, estimating area-based traits directly was usually more accurate than multiplying mass-based estimates by LMA estimates, especially for traits distributed in proportion to area (Table S1). This consideration is important given that many research questions may require traits expressed on an area basis.

Using transmittance or absorbance spectra instead of reflectance spectra increases accuracy for most traits, but only slightly (Table S2). It may be relevant that the traits that show the greatest improvement include most of the highly area-proportional traits. Given that transmittance or absorbance spectra yielded little improvement for most traits, adding transmittance measurements may not aid much in trait estimation, although they are still useful in endeavors like radiative transfer modeling (Spafford *et al.*, 2021).

### External validation and model transferability

Aside from our internal validation, we also considered model performance under less ideal scenarios: we tested the primary models on external validation datasets, and built another set of models to be tested on a functional group left out during their construction. When transferring models to left-out functional groups, performance was usually worse (lower  $R^2$ , higher %RMSE<sub>full</sub>) than when models were evaluated on a random internal validation dataset (Fig. 6; Table S5). This finding is consistent with previous studies transferring models among species (Helsen *et al.*, 2021) or sites (Yan *et al.*, 2021). In general, trait models performed worse when the trait distributions in the calibration and validation datasets were less similar, but the strength and even the direction of the trend varied among traits (Fig. 6b). Thus, support for Hypothesis 1 was equivocal. Predictions of LMA



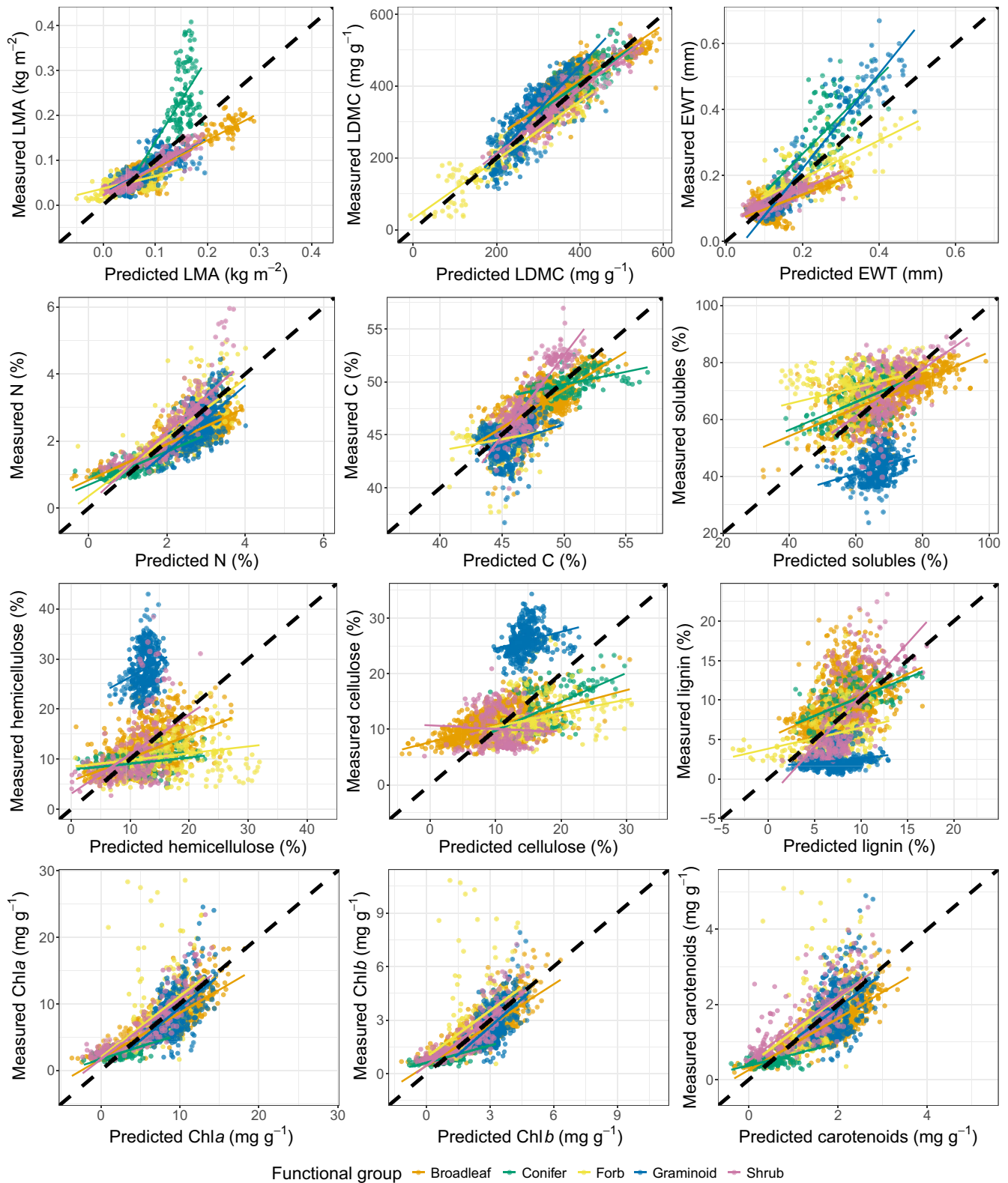


**Fig. 7** Plots of observations against reflectance-based partial least-squares regression predictions from model transferability analyses for various leaf chemical and structural traits. Here, we estimated traits for samples of each functional group from models calibrated on all the remaining functional groups; within panels, predictions for each functional group come from separately trained models. The black dashed line in each panel is the 1 : 1 line. Colored lines represent best-fit lines from ordinary least squares (OLS) regression for each functional group. EWT, equivalent water thickness; LDMC, leaf dry matter content; LMA, leaf mass per area.

among conifers and carbon fractions among graminoids were strongly biased and failed to capture the functional distinctiveness of these groups. These results underscore that models must be built using samples whose diversity encompasses the models' expected domain of application (Yang *et al.*, 2016; Schweiger, 2020; Beauchamp-Rioux, 2022).

The external validation was a more severe test of model generality because the data were collected on different species with different instruments using different trait measurement protocols. This kind of scenario may represent a more realistic use case for such models. All traits showed declines in performance from internal to external validation (Table 2). This result is expected and consistent with previous findings: for example, Serbin *et al.*'s (2019) global model of LMA showed  $R^2 = 0.89$  for internal validation and 0.66 for external validation on LOPEX and ANGERS, as compared with  $R^2 = 0.89$  (internal) and 0.59 (external, averaged across datasets) here. On our data, the Serbin *et al.*'s (2019) model shows fairly good performance ( $R^2 = 0.680$ ; RMSE = 0.036; %RMSE = 17.5%), but with a strong bias toward underpredicting LMA of conifers and the graminoid *Eriophorum vaginatum* L. and a slight bias toward overpredicting LMA of most other plants (Fig. S22). These results further underscore the challenges that arise when transferring models among settings and instruments.

The rank order of  $R^2$  across traits was broadly similar between the internal validation, external validation, and model transferability analyses (Fig. 6a), which offers some general support for Hypothesis 2. Models for LMA, LDMC, and EWT performed relatively well in all analyses, while models for most macronutrients and micronutrients performed poorly in both internal and external validation (but were not included in model transferability analyses). Pigments, N, C, and carbon fractions were generally intermediate. However, in both the external validation and model transferability analyses, C and carbon fractions showed particularly strong declines in  $R^2$  compared to internal validation (Fig. 6a). Dry matter components such as cellulose and lignin are associated mainly with weak absorption features throughout the NIR and SWIR (Curran, 1989). By contrast, traits without such strong declines – LMA, LDMC, EWT, N, and pigments – have stronger influences on the spectrum, enough that most are incorporated into mechanistic models like PROSPECT (Féret *et al.*, 2008). This contrast could imply that models are most transferable when their target traits have strong absorption features. Many chemical traits may be estimated more reliably using spectra of pressed or ground leaves, which by removing the water absorption features expose the subtler features of dry matter components (Kothari *et al.*, 2023).

Even though our estimates of LMA and EWT correlated well with measured values in the external validation, they also had a strong bias toward overestimation (Fig. 5), which could complicate their use in practice. This bias may have resulted from varying measurement protocols, or from differences in instrumentation that can have a subtle but pervasive influence on the measured spectra (Castro-Esau *et al.*, 2006; Lukeš *et al.*, 2017; Hovi *et al.*, 2018). This bias could perhaps be corrected by measuring a subset of trait values to determine how they

correspond to model predictions, and then transforming the remaining predictions accordingly. In the longer term, it might become easier to get accurate trait estimates using existing models if techniques are developed to reconcile differences among instruments (Meireles *et al.*, 2020; Schweiger, 2020). Deep learning approaches like convolutional neural networks may also address this problem through their greater flexibility and capacity for transfer learning (Kattenborn *et al.*, 2021).

### Implications for global trait-spectra modeling

Our models draw from samples representing several functional groups and a wide range of temperate ecosystems, including wetlands, grasslands, and closed-canopy forests (Table 1). However, these samples represent just a portion of Earth's vast plant diversity – omitting, for example, tundra, drylands, and tropical biomes. These biomes would surely contain combinations of optically important traits missing in our dataset, which would need to be represented in a universal model that could be used in mapping functional trait variation worldwide. Likewise, we focus on sunlit leaves, but the relationships we find between traits and spectra may generalize poorly to shade leaves (Yang *et al.*, 2016). We hope plant ecologists can use our data and models not only as a tool to address ecological questions, but also as a foundation for building yet more general models.

Our results imply that some traits can consistently be estimated better than others. We can compare our findings with Asner *et al.* (2011), who measured a similar set of traits on a vast number of samples from canopy leaves in humid tropical forests. The two studies are broadly consistent despite representing disparate subsets of the world's plant diversity. Both found that models for LMA and water content were most accurate ( $R^2 > 0.85$ ), followed by, in varying orders, C and N, pigments, and carbon fractions ( $R^2 = 0.55$ – $0.85$ ). In both studies, models for other elements were typically worse ( $R^2 < 0.65$ ), but better for Ca and K than many other elements. Both studies also found that transmittance spectra yielded slightly better performance for most traits. The stability in rankings suggests a general hierarchy of traits that are the most practical targets for reliable model-based estimation.

The emerging body of research showing that spectral models can yield fast, reliable estimates of many leaf traits across functional groups, and ecosystems could expand our ability to map and monitor plant function around the world. Because leaf spectra are among the dominant influences on canopy spectra (Baret *et al.*, 1994), understanding the relationship between traits and spectra at the leaf level is a foundation for doing so at the canopy level. When a leaf trait cannot be estimated from leaf spectra, it may also be infeasible to estimate it from canopy spectra except perhaps through covariance with canopy structure (Kothari & Schweiger, 2022), or in those cases where multiple scattering within canopies enhances chemical absorption features (Baret *et al.*, 1994).

In more practical terms, leaf-level spectral trait estimates may serve to help bridge the gap in scale between conventional trait measurements and remote sensing of plant function. For

example, trait estimates based on leaf-level empirical models have higher throughput than conventional measurements, making them useful for training canopy-level empirical models (Singh *et al.*, 2015; Wang *et al.*, 2020). As drone-based sensors approach the spatial resolution of individual leaves (Arroyo-Mora *et al.*, 2019), it may even become feasible to apply leaf-level models directly to image pixels. The potential development of general leaf-level empirical models also suggests the prospect of combining them with canopy RTMs. Inverting canopy RTMs allows the estimation of leaf spectra, and canopy models are often coupled with leaf RTMs like PROSPECT to further estimate leaf traits (Jacquemoud *et al.*, 2009). However, using leaf-level empirical models rather than leaf RTMs could allow more flexibility to predict a wider range of traits. As increasing volumes of remotely sensed data arrive from drones, airborne sensors, and satellites, the task of scaling between point measurements on the ground and continuous canopy imagery will surely grow in importance.

Our findings clarify both the opportunities and challenges of using spectral trait estimates. Research has not yet progressed to the point where plant ecologists can use existing empirical models to estimate traits in their study systems without further validation. Aside from the issues of taxonomic and functional representativeness, our external validation underscores the challenge of transferring models among instruments. If models are limited in their scope to particular instruments, taxa, or ecosystems, the result may be an undesirable proliferation of models, selecting among which requires specialized knowledge. Overcoming these issues may require data synthesis across taxa and ecosystems and new methodological developments to reconcile data across instruments. Even setting these issues aside, some aspects of leaf function (e.g. elemental composition) may remain hard to measure accurately based on spectroscopy alone. We hope that the promise of rapid, large-scale monitoring of plant function inspires the coordinated effort needed to understand and (when possible) overcome these challenges.

In sum, we built models to predict traits from reflectance spectra using nearly 2000 leaf samples from 103 species. Traits varied a great deal in how well they could be estimated using spectral models. Our models for structural and water-related traits were very accurate in internal validation and showed great promise in external validation; by contrast, our models for many micronutrients performed very poorly. We suggest that these patterns reflect a general hierarchy that emerges mainly from the varying degrees of influence these traits have on the spectrum. Leaf reflectance spectra thus bear the imprint of many aspects of leaf function – but not all to the same degree. Most importantly, we show that many traits can be estimated accurately from spectra using general models that span multiple functional groups and ecosystems. This finding represents a significant advance in leveraging spectra toward major goals in functional ecology.

## Acknowledgements

We conducted this research at institutions and field sites located on the largely unceded ancestral and contemporary land of many

First Nations and Aboriginal people. We thank Jocelyne Ayotte, Zachary Bélisle, Fabien Cichonski, Chris Colton, Myriam Cloutier, Aurélie Dessain, Vincent Fournier, Juliette Frappier-Lecomte, Isabelle Gareau, Sam Grubinger, Elisabeth Hardy-Lachance, Sandra Jooty, Alexandra Massey, Antoine Mathieu, Chris Mulverhill, Rime Néron, Florence Normand-Boisseau, Clément Robert-Bigras, Sabine St-Jean, Guillaume Tougas, Charlotte Taillefer, Francois du Toit, and Madeleine Trickey-Massé for their help with field sampling and laboratory analyses. We thank the National Capital Commission, the Société des établissements de plein air du Québec, the Station de biologie des Laurentides of Université de Montréal, the Jardin botanique de Montréal, the Institut de recherche d'Hydro-Québec, the Nature Conservancy of Canada, and the Parks and Wildlife Service of Western Australia for permissions to conduct sampling and for lending the ecological and logistical expertise of their staff. We also thank the many members of CABO who have helped to strengthen this work through their stimulating comments and questions. CABO was funded by a Discovery Frontiers grant to EL, MK, AB, MV and NCC from the Natural Sciences and Engineering Research Council of Canada (NSERC; #509190-2017) with additional support to EL from the Canada Foundation for Innovation (#37132, #35472) and Université de Montréal. RB-R, FB and ALC were supported by student scholarships from NSERC, and XG-M by the Fonds de recherche du Québec – Nature et Technologies (FRQNT).













## Competing interests

None declared.

## Author contributions

SK and EL designed the project with contributions from AB, NCC, MK and MV. RB-R, FB, ALC, AG, XG-M, PWH, JP, AKS and SD-T collected and curated the spectral and trait data. SK analyzed the data, interpreted the results, and wrote the first draft with substantial contributions from EL. All authors contributed to further revisions of the paper.

## ORCID

Rosalie Beauchamp-Rioux  <https://orcid.org/0000-0002-6461-7646>  
 Anne Bruneau  <https://orcid.org/0000-0001-5547-0796>  
 Nicholas C. Coops  <https://orcid.org/0000-0002-0151-9037>  
 Anna L. Crofts  <https://orcid.org/0000-0002-0098-1844>  
 Xavier Guilbeault-Mayers  <https://orcid.org/0000-0002-4465-2153>  
 Paul W. Hacker  <https://orcid.org/0000-0001-9786-3715>  
 Margaret Kalacska  <https://orcid.org/0000-0002-1676-481X>  
 Shan Kothari  <https://orcid.org/0000-0001-9445-5548>  
 Etienne Laliberté  <https://orcid.org/0000-0002-3167-2622>  
 Juliana Pardo  <https://orcid.org/0000-0002-6950-8246>  
 Anna K. Schweiger  <https://orcid.org/0000-0002-5567-4200>  
 Mark Vellend  <https://orcid.org/0000-0002-2491-956X>



## Data availability

All fresh-leaf spectral data used in calibration and internal validation are available through the CABO data portal (<https://data.caboscience.org/leaf/>), and the spectral and trait data are also archived on EcoSIS (Kothari *et al.*, 2022a). Spectral and trait data from the Dessain project used in external validation are archived on EcoSIS (Kothari *et al.*, 2022c). The primary models based on reflectance (with mass- and area-based traits), transmittance, and absorbance spectra are archived along with instructions for using them on Borealis (Kothari *et al.*, 2022b). Spectral processing and analysis scripts are available as a repository on GitHub (<https://github.com/ShanKothari/CABO-trait-models>), and the specific version used for this manuscript is also archived at Zenodo (Kothari, 2022).

## References

- American Society for Testing and Materials. 2020. *Standard tables for reference solar spectral irradiances: direct normal and hemispherical on 37° tilted surface (standard G173-03)*. doi: 10.1520/G0173-03R20.
- Arroyo-Mora JP, Kalacska M, Inamdar D, Soffer R, Lucanus O, Gorman J, Naprstek T, Schaaf ES, Ifimov G, Elmer K *et al.* 2019. Implementation of a UAV-hyperspectral pushbroom imager for ecological monitoring. *Drones* 3: 12.
- Asner GP, Martin RE, Knapp DE, Tupayachi R, Anderson C, Carranza L, Martinez P, Houcheime M, Sinca F, Weiss P. 2011. Spectroscopy of canopy chemicals in humid tropical forests. *Remote Sensing of Environment* 115: 3587–3598.
- Baret F, Vanderbilt VC, Steven MD, Jacquemoud S. 1994. Use of spectral analogy to evaluate canopy reflectance sensitivity to leaf optical properties. *Remote Sensing of Environment* 48: 253–260.
- Beauchamp-Rioux R. 2022. *Les effets de l'environnement et de la phénologie sur les propriétés spectrales foliaires d'arbres des forêts tempérées*. MSc thesis, Université de Montréal, Montréal, QC, Canada.
- Burnett AC, Anderson J, Davidson KJ, Ely KS, Lamour J, Li Q, Morrison BD, Yang D, Rogers A, Serbin SP. 2021. A best-practice guide to predicting plant traits from leaf-level hyperspectral data using partial least squares regression. *Journal of Experimental Botany* 72: 6175–6189.
- Castro-Esau KL, Sánchez-Azofeifa GA, Rivard B. 2006. Comparison of spectral indices obtained using multiple spectroradiometers. *Remote Sensing of Environment* 103: 276–288.
- Cavender-Bares J, Gamon JA, Hobbie SE, Madritch MD, Meireles JE, Schweiger AK, Townsend PA. 2017. Harnessing plant spectra to integrate the biodiversity sciences across biological and spatial scales. *American Journal of Botany* 104: 966–969.
- Chadwick KD, Asner GP. 2016. Organismic-scale remote sensing of canopy foliar traits in lowland tropical forests. *Remote Sensing* 8: 87.
- Chadwick KD, Asner GP. 2018. Landscape evolution and nutrient rejuvenation reflected in Amazon forest canopy chemistry. *Ecology Letters* 21: 978–988.
- Chavana-Bryant C, Malhi Y, Wu J, Asner GP, Anastasiou A, Enquist BJ, Cosio Caravani EG, Doughty CE, Saleska SR, Martin RE *et al.* 2017. Leaf aging of Amazonian canopy trees as revealed by spectral and physiochemical measurements. *New Phytologist* 214: 1049–1063.
- Cornwell WK, Cornelissen JHC, Amatangelo K, Dorrepaal E, Eviner VT, Godoy O, Hobbie SE, Hoores B, Kurokawa H, Pérez-Harguindeguy N *et al.* 2008. Plant species traits are the predominant control on litter decomposition rates within biomes worldwide. *Ecology Letters* 11: 1065–1071.
- Couture JJ, Singh A, Rubert-Nason KF, Serbin SP, Lindroth RL, Townsend PA. 2016. Spectroscopic determination of ecologically relevant plant secondary metabolites. *Methods in Ecology and Evolution* 7: 1402–1412.
- Curran PJ. 1989. Remote sensing of foliar chemistry. *Remote Sensing of Environment* 30: 271–278.
- Durán SM, Martin RE, Díaz S, Maitner BS, Malhi Y, Salinas N, Shenkin A, Silman MR, Wiczynski DJ, Asner GP *et al.* 2019. Informing trait-based ecology by assessing remotely sensed functional diversity across a broad tropical temperature gradient. *Science Advances* 5: eaaw8114.
- Ely KS, Burnett AC, Lieberman-Cribbin W, Serbin SP, Rogers A. 2019. Spectroscopy can predict key leaf traits associated with source–sink balance and carbon–nitrogen status. *Journal of Experimental Botany* 70: 1789–1799.
- Féret J-B, Berger K, de Boissieu F, Malenovský Z. 2021. PROSPECT-PRO for estimating content of nitrogen-containing leaf proteins and other carbon-based constituents. *Remote Sensing of Environment* 252: 112173.
- Féret J-B, François C, Asner GP, Gitelson AA, Martin RE, Bidet LPR, Ustin SL, le Maire G, Jacquemoud S. 2008. PROSPECT-4 and 5: advances in the leaf optical properties model separating photosynthetic pigments. *Remote Sensing of Environment* 112: 3030–3043.
- Féret J-B, Gitelson AA, Noble SD, Jacquemoud S. 2017. PROSPECT-D: towards modeling leaf optical properties through a complete lifecycle. *Remote Sensing of Environment* 193: 204–215.
- Féret J-B, le Maire G, Jay S, Berveiller D, Bendoula R, Hmimina G, Cheriai A, Oliveira JC, Ponzoni FJ, Solanki T *et al.* 2019. Estimating leaf mass per area and equivalent water thickness based on leaf optical properties: potential and limitations of physical modeling and machine learning. *Remote Sensing of Environment* 231: 110959.
- Frye HA, Aiello-Lammens ME, Euston-Brown D, Jones CS, Mollmann HK, Merow C, Slingsby JA, van der Merwe H, Wilson AM, Silander JA. 2021. Plant spectral diversity as a surrogate for species, functional and phylogenetic diversity across a hyper-diverse biogeographic region. *Global Ecology and Biogeography* 30: 1403–1417.
- Funk JL, Larson JE, Ames GM, Butterfield BJ, Cavender-Bares J, Firn J, Laughlin DC, Sutton-Grier AE, Williams L, Wright J. 2017. Revisiting the Holy Grail: using plant functional traits to understand ecological processes. *Biological Reviews* 92: 1156–1173.
- Girard A, Schweiger AK, Carteron A, Kalacska M, Laliberté E. 2020. Foliar spectra and traits of bog plants across nitrogen deposition gradients. *Remote Sensing* 12: 2448.
- Grossman YL, Ustin SL, Jacquemoud S, Sanderson EW, Schmuck G, Verdebout J. 1996. Critique of stepwise multiple linear regression for the extraction of leaf biochemistry information from leaf reflectance data. *Remote Sensing of Environment* 56: 182–193.
- Guzmán Q JA, Sánchez-Azofeifa GA. 2021. Prediction of leaf traits of lianas and trees via the integration of wavelet spectra in the visible-near infrared and thermal infrared domains. *Remote Sensing of Environment* 259: 112406.
- Hacker PW, Coops NC, Laliberté E, Michaletz ST. 2022. Variations in accuracy of leaf functional trait prediction due to spectral mixing. *Ecological Indicators* 136: 108687.
- Helsen K, Bassi L, Feilhauer H, Kattenborn T, Matsushima H, Van Cleemput E, Somers B, Honnay O. 2021. Evaluating different methods for retrieving intraspecific leaf trait variation from hyperspectral leaf reflectance. *Ecological Indicators* 130: 108111.
- Hosgood B, Jacquemoud S, Andreoli G, Verdebout J, Pedrini G, Schmuck G. 1994. *Leaf Optical Properties Experiment 93 (EUR 16905 EN)*. Luxembourg City, Luxembourg: European Commission, Institute for Remote Sensing Applications – Joint Research Centre.
- Hovi A, Forsström P, Möttö M, Rautiainen M. 2018. Evaluation of accuracy and practical applicability of methods for measuring leaf reflectance and transmittance spectra. *Remote Sensing* 10: 25.
- Jacquemoud S, Ustin S. 2019. *Leaf optical properties*. Cambridge, UK: Cambridge University Press.
- Jacquemoud S, Verhoef W, Baret F, Bacour C, Zarco-Tejada PJ, Asner GP, François C, Ustin SL. 2009. PROSPECT+SAIL models: a review of use for vegetation characterization. *Remote Sensing of Environment* 113: S56–S66.
- Kattenborn T, Leitloff J, Schiefer F, Hinz S. 2021. Review on convolutional neural networks (CNN) in vegetation remote sensing. *ISPRS Journal of Photogrammetry and Remote Sensing* 173: 24–49.
- Kattenborn T, Schiefer F, Zarco-Tejada P, Schmidtlein S. 2019. Advantages of retrieving pigment content [ $\mu\text{g}/\text{cm}^2$ ] versus concentration [%] from canopy reflectance. *Remote Sensing of Environment* 230: 111195.



- Kattge J, Bönisch G, Díaz S, Lavorel S, Prentice IC, Leadley P, Tautenhahn S, Werner GDA, Aakala T, Abedi M *et al.* 2020. TRY plant trait database – enhanced coverage and open access. *Global Change Biology* 26: 119–188.
- Kothari S. 2022. ShanKothari/CABO-trait-models: CABO Trait Modeling code (v.0.0.2). *Zenodo*. doi: [10.5281/zenodo.7308839](https://doi.org/10.5281/zenodo.7308839).
- Kothari S, Beauchamp-Rioux R, Blanchard F, Crofts AL, Girard A, Guilbeault-Mayers X, Hacker PW, Pardo J, Schweiger AK, Demers-Thibeault S *et al.* 2022a. CABO 2018–2019 leaf-level spectra [Data set]. *EcoSIS*. doi: [10.21232/44VXHORW](https://doi.org/10.21232/44VXHORW).
- Kothari S, Beauchamp-Rioux R, Blanchard F, Crofts AL, Girard A, Guilbeault-Mayers X, Hacker PW, Pardo J, Schweiger AK, Demers-Thibeault S *et al.* 2022b. Models for predicting leaf traits across functional groups using reflectance spectroscopy [Data set]. *Borealis*. doi: [10.5683/SP3/NYABAG](https://doi.org/10.5683/SP3/NYABAG).
- Kothari S, Dessain A, Beauchamp-Rioux R, Blanchard F, Crofts AL, Girard A, Guilbeault-Mayers X, Hacker PW, Pardo J, Schweiger AK *et al.* 2022c. Dessain project reflectance spectra [Data set]. *EcoSIS*. doi: [10.21232/VYJzNBEy](https://doi.org/10.21232/VYJzNBEy).
- Kothari S, Beauchamp-Rioux R, Laliberté E, Cavender-Bares J. 2023. Reflectance spectroscopy allows rapid, accurate, and non-destructive estimates of functional traits from pressed leaves. *Methods in Ecology and Evolution* 14: 385–401.
- Kothari S, Schweiger A. 2022. Plant spectra as integrative measures of plant phenotypes. *Journal of Ecology* 110: 2536–2554.
- Kunster G, Falster D, Coomes DA, Hui F, Kooyman RM, Laughlin DC, Poorter L, Vanderwel M, Vieilledent G, Wright SJ *et al.* 2016. Plant functional traits have globally consistent effects on competition. *Nature* 529: 204–207.
- Lukeš P, Homolová L, Navrátil M, Hanuš J. 2017. Assessing the consistency of optical properties measured in four integrating spheres. *International Journal of Remote Sensing* 38: 3817–3830.
- Meireles JE, Cavender-Bares J, Townsend PA, Ustin S, Gamon JA, Schweiger AK, Schaepman ME, Asner GP, Martin RE, Singh A *et al.* 2020. Leaf reflectance spectra capture the evolutionary history of seed plants. *New Phytologist* 228: 485–493.
- Mevik B-H, Wehrens R, Liland KH. 2019. *PLS: partial least squares and principal component regression*. R package v.2.7-1. [WWW document] URL <https://CRAN.R-project.org/package=pls>
- Nunes MH, Davey MP, Coomes DA. 2017. On the challenges of using field spectroscopy to measure the impact of soil type on leaf traits. *Biogeosciences* 14: 3371–3385.
- Ollinger SV, Richardson AD, Martin ME, Hollinger DY, Frolking SE, Reich PB, Plourde LC, Katul GG, Munger JW, Oren R *et al.* 2008. Canopy functional, carbon assimilation, and albedo in temperate and boreal forests: functional relations and potential climate feedbacks. *Proceedings of the National Academy of Sciences, USA* 105: 19336–19341.
- Osnas JLD, Lichstein JW, Reich PB, Pacala SW. 2013. Global leaf trait relationships: mass, area, and the leaf economics spectrum. *Science* 340: 741–744.
- Pardo MJ. 2021. *Foliar spectra accurately distinguish the invasive common reed from co-occurring plant species throughout a growing season*. MSc thesis, Université de Montréal, Montréal, QC, Canada.
- Pérez-Harguindeguy N, Díaz S, Garnier E, Lavorel S, Poorter H, Jaureguiberry P, Bret-Harte MS, Cornwell WK, Craine JM, Gurvich DE *et al.* 2013. New handbook for standardised measurement of plant functional traits worldwide. *Australian Journal of Botany* 61: 167–234.
- Poncet P, R Core Team. 2019. *STATIP: statistical functions for probability distributions and regression*. R package v.0.2.3. [WWW document] URL <https://CRAN.R-project.org/package=statip>
- Pullanagari RR, Dehghan-Shoar M, Yule IJ, Bhatia N. 2021. Field spectroscopy of canopy nitrogen concentration in temperate grasslands using a convolutional neural network. *Remote Sensing of Environment* 257: 112353.
- R Core Team. 2020. *R: a language and environment for statistical computing*. Vienna, Austria: R Foundation for Statistical Computing. [WWW document] URL <https://www.R-project.org/> [accessed 9 March 2020].
- Richardson AD, Duigan SP, Berlyn GP. 2002. An evaluation of noninvasive methods to estimate foliar chlorophyll content. *New Phytologist* 153: 185–194.
- Schweiger AK. 2020. Spectral field campaigns: planning and data collection. In: Cavender-Bares J, Gamon JA, Townsend PA, eds. *Remote sensing of plant biodiversity*. Cham, Switzerland: Springer, 385–423.
- Schweiger AK, Cavender-Bares J, Townsend PA, Hobbie SE, Madritch MD, Wang R, Tilman D, Gamon JA. 2018. Plant spectral diversity integrates functional and phylogenetic components of biodiversity and predicts ecosystem function. *Nature Ecology & Evolution* 2: 976–982.
- Serbin SP, Singh A, McNeil BE, Kingdon CC, Townsend PA. 2014. Spectroscopic determination of leaf morphological and biochemical traits for northern temperate and boreal tree species. *Ecological Applications* 24: 1651–1669.
- Serbin SP, Wu J, Ely KS, Kruger EL, Townsend PA, Meng R, Wolfe BT, Chlus A, Wang Z, Rogers A. 2019. From the Arctic to the tropics: multi-biome prediction of leaf mass per area using leaf reflectance. *New Phytologist* 224: 1557–1568.
- Sims DA, Gamon JA. 2002. Relationships between leaf pigment content and spectral reflectance across a wide range of species, leaf structures and developmental stages. *Remote Sensing of Environment* 81: 337–354.
- Singh A, Serbin SP, McNeil BE, Kingdon CC, Townsend PA. 2015. Imaging spectroscopy algorithms for mapping canopy foliar chemical and morphological traits and their uncertainties. *Ecological Applications* 25: 2180–2197.
- Spafford L, le Maire G, MacDougall A, de Boissieu F, Féret J-B. 2021. Spectral subdomains and prior estimation of leaf structure improves PROSPECT inversion on reflectance or transmittance alone. *Remote Sensing of Environment* 252: 112176.
- Turner BL, Hayes PE, Laliberté E. 2018. A climosequence of chronosequences in southwestern Australia. *European Journal of Soil Science* 69: 69–85.
- Wang S, Guan K, Wang Z, Ainsworth EA, Zheng T, Townsend PA, Li K, Moller C, Wu G, Jiang C. 2021. Unique contributions of chlorophyll and nitrogen to predict crop photosynthetic capacity from leaf spectroscopy. *Journal of Experimental Botany* 72: 341–354.
- Wang Z, Chlus A, Geygan R, Ye Z, Zheng T, Singh A, Couture JJ, Cavender-Bares J, Kruger EL, Townsend PA. 2020. Foliar functional traits from imaging spectroscopy across biomes in eastern North America. *New Phytologist* 228: 494–511.
- Wang Z, Skidmore AK, Darvishzadeh R, Wang T. 2018. Mapping forest canopy nitrogen content by inversion of coupled leaf-canopy radiative transfer models from airborne hyperspectral imagery. *Agricultural and Forest Meteorology* 253–254: 247–260.
- Wessman CA, Aber JD, Peterson DL, Melillo JM. 1988. Remote sensing of canopy chemistry and nitrogen cycling in temperate forest ecosystems. *Nature* 335: 154–156.
- Wold S, Sjöström M, Eriksson L. 2001. PLS-regression: a basic tool of chemometrics. *Chemometrics and Intelligent Laboratory Systems* 58: 109–130.
- Yan Z, Guo Z, Serbin SP, Song G, Zhao Y, Chen Y, Wu S, Wang J, Wang X, Li J *et al.* 2021. Spectroscopy outperforms leaf trait relationships for predicting photosynthetic capacity across different forest types. *New Phytologist* 232: 134–147.
- Yang X, Tang J, Mustard JF, Wu J, Zhao K, Serbin S, Lee J-E. 2016. Seasonal variability of multiple leaf traits captured by leaf spectroscopy at two temperate deciduous forests. *Remote Sensing of Environment* 179: 1–12.
- Zheng Z, Zeng Y, Schneider FD, Zhao Y, Zhao D, Schmid B, Schaepman ME, Morsdorf F. 2021. Mapping functional diversity using individual tree-based morphological and physiological traits in a subtropical forest. *Remote Sensing of Environment* 252: 112170.

## Supporting Information

Additional Supporting Information may be found online in the Supporting Information section at the end of the article.

**Fig. S1** Comparison of reflectance-based model performance under trait transformations.

**Fig. S2** Principal components analysis of traits.

**Fig. S3** Reflectance, transmittance, and absorbance spectra separated by functional group.

**Fig. S4** Comparisons of measurements and predictions for structural and water-related traits.

**Fig. S5** Comparisons of measurements and predictions for major elemental nutrients.

**Fig. S6** Comparisons of measurements and predictions for carbon fractions.

**Fig. S7** Comparisons of measurements and predictions for pigments.

**Fig. S8** Comparisons of measurements and predictions for ICP-OES elements (part one).

**Fig. S9** Comparisons of measurements and predictions for ICP-OES elements (part two).

**Fig. S10** Comparisons of measurements and predictions for ICP-OES elements (part three).

**Fig. S11** Distributions of reflectance-based model performance statistics from jackknife analyses.

**Fig. S12** Distributions of transmittance-based model performance statistics from jackknife analyses.

**Fig. S13** Distributions of absorptance-based model performance statistics from jackknife analyses.

**Fig. S14** The variable influence on projection metric for reflectance-based models.

**Fig. S15** The variable influence on projection metric for transmittance-based models.

**Fig. S16** The variable influence on projection metric for absorptance-based models.

**Fig. S17** Comparisons of measurements and predictions for reflectance-based models of area-normalized traits, excluding ICP-OES elements.

**Fig. S18** Comparisons of measurements and predictions for reflectance-based models of area-normalized ICP-OES elements.

**Fig. S19** Distributions of reflectance-based model performance statistics for area-normalized traits from jackknife analyses.

**Fig. S20** The variable influence on projection metric for reflectance-based models to predict area-normalized traits.

**Fig. S21** Comparisons of measurements and predictions in external validation for ICP-OES elements.

**Fig. S22** Comparisons of measurements of leaf mass per area and predictions made using Serbin *et al.* (2019)'s models.

**Methods S1** Details of spectral and trait measurements for the main CABO dataset.

**Methods S2** Details of external validation.

**Table S1** Summary statistics of models predicting area-normalized traits from reflectance spectra.

**Table S2** Comparisons of summary statistics for models predicting traits from reflectance, transmittance, and absorptance spectra.

**Table S3** Summary statistics of external validation using models trained on continuum-removed spectra.

**Table S4** Summary statistics of external validation using models trained on brightness-normalized spectra.

**Table S5** Summary statistics from model transferability analyses among functional groups.

Please note: Wiley is not responsible for the content or functionality of any Supporting Information supplied by the authors. Any queries (other than missing material) should be directed to the *New Phytologist* Central Office.